



Cullinan, J., Wisnom, M., & Bond, I. (2015). *Optimised vascular systems for the in-situ repair of composite T-joints*. Paper presented at 20th International Conference on Composite Materials (ICCM20), Copenhagen, Denmark.

Peer reviewed version

[Link to publication record in Explore Bristol Research](#)  
PDF-document

## University of Bristol - Explore Bristol Research

### General rights

This document is made available in accordance with publisher policies. Please cite only the published version using the reference above. Full terms of use are available:  
<http://www.bristol.ac.uk/red/research-policy/pure/user-guides/ebr-terms/>



a method for the introduction of optimised repair *infrastructure* into a complex composite structure. The specific objectives of implementing self-healing technologies into composite structures are twofold; to increase the allowable damage limit (ADL) for the structure and to increase the safe load bearing capability of structures with sub-critical damage (see Fig. 2).

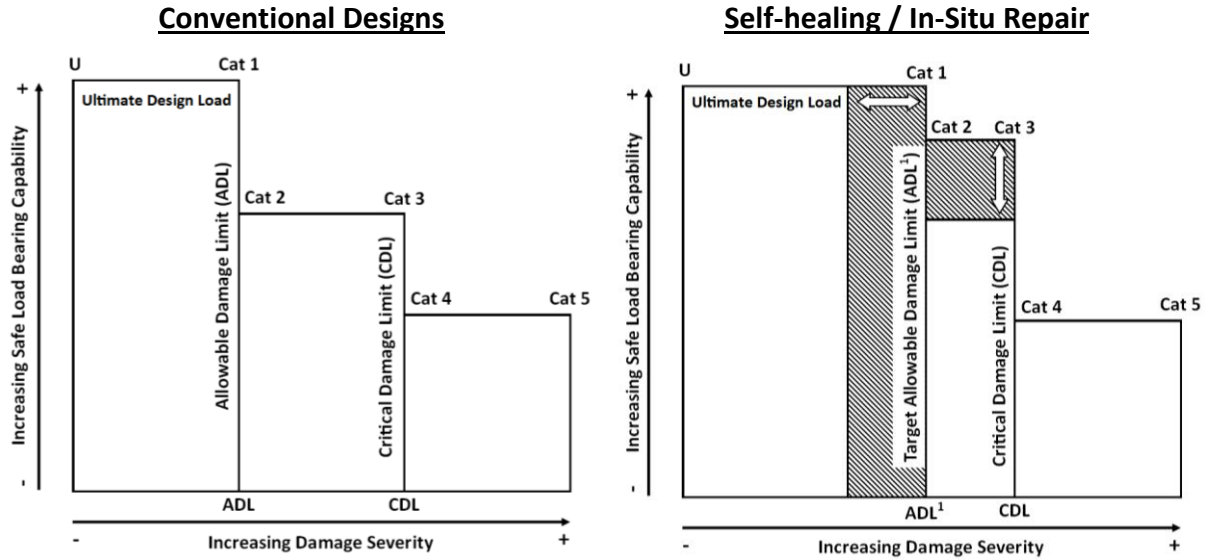


Figure 2: Increased allowable damage limits (ADLs) and residual load bearing capabilities to be achieved through the use of self-healing technologies. Cat 1 – BVID & allowable manufacturing defects (no repair), Cat 2 – Sub-critical VID (repair during normal inspection cycle), Cat 3 – Critical VID (repair soon after occurrence), Cat 4 – Obvious to users requiring repair after occurrence, Cat 5 – Major damage, immediate repair required. (Adapted from [2])

A number of methods have been proposed for implementing self-healing in composite materials. These can be broadly grouped into three different strategies; discrete *capsule-based* [3–6] systems, continuous or semi-continuous *vascular* [7–9] systems and *intrinsic* [10,11] systems. Both capsule-based and vascular systems rely on the rupturing of resin filled vessels, which can leach into the damage plane and restore functionality. Intrinsic systems rely instead on the chemical affinity of the damaged surfaces to self-adhere, typically through strong secondary electro-chemical bonding. Although all three of these strategies have been established in bulk polymeric materials, the presence of the fibre reinforcement phase provides challenges in implementing self-healing in FRPs.

Focusing on vascular systems, some of these challenges have been examined by Norris *et al* [12–16]. It has been found that the location and size of the embedded vasculs, as well as their orientation relative to the fibre reinforcement, needs to be carefully controlled in order to optimise self-healing performance. A key finding was that it is highly preferable to align vasculs in the fibre direction, as transverse or oblique vasculature requires undesirable discontinuities to be introduced into the fibre architecture [14].

The T-joint configuration was selected for investigation as it is commonly used in many structural applications and is itself a good lab-scale analogue for more complex structures. The deltoid region, as shown in Fig. 1, is a region of unidirectional (UD) material used to maintain the form and integrity of the joint. This region has been shown to be highly susceptible to both manufacturing defects [17] and damage during mechanical loading [18,19]. The presence of UD deltoid material, combined with the geometric complexity and susceptibility to damage make it an ideal candidate for the deployment of an in-situ repair strategy. It has been shown previously by the authors that the introduction of circular vasculature into the deltoid region results in a reduction in mechanical performance [20]. The work presented herein aims to mitigate the detrimental influence of vasculature on the mechanical performance of T-joints, through the optimisation of the vasculature topology and positioning.

## 2 EXPERIMENTAL

### 2.1 2D Plane Strain Model

A plane strain analysis was performed using Abaqus/CAE 6.12 to determine the influence of vasculature on T-joint strength and failure initiation location. The methodology employed here was identical to that used previously by Cullinan *et al.* [20]. A brief overview has been included here for completeness. A uniform vertical displacement (U2) of 2mm was applied to the top of the web section as shown in Fig. 1. The rollers were modelled by applying a vertical displacement constraint (U2=0) at the corner nodes of the overlamine. Thermal loading of -160°C (180°C cure, 20°C T<sub>amb</sub>) was applied to the entirety of the model. The small resin pockets at the vertices of the deltoid region were modelled as fiber reinforced regions as these regions were deemed to have no influence on the global stress state.

<i>IM7/8552 Properties</i>			
$E_{11} = 161 \text{ GPa}$	$\nu_{12} = \nu_{13} = 0.32$	$G_{12} = G_{13} = 5.17 \text{ GPa}$	$\alpha_{11} = 0 \times 10^{-6}/^{\circ}\text{C}$
$E_{22} = E_{33} = 11.38 \text{ GPa}$	$\nu_{23} = 0.436$	$G_{23} = 3.98 \text{ GPa}$	$\alpha_{22} = \alpha_{33} = 30 \times 10^{-6}/^{\circ}\text{C}$

Table 1. Thermoelastic properties of IM7/8552 [21]

$l_s$ (mm)	$b$ (mm)	$h$ (mm)	<i>Ply Orientation</i>		
			<i>Substrate</i>	<i>Overlamine</i>	<i>Deltoid</i>
100	20	40	$[0^{\circ}/-45^{\circ}/90^{\circ}/45^{\circ}]_{3S}$	$[(0^{\circ}/-45^{\circ}/90^{\circ}/45^{\circ})_2/0^{\circ}]_S$	$90^{\circ}$

Table 2. Model dimensions and ply orientations (see Fig. 1)

Plyies were modelled individually with two elements per ply. Off axis plyies (i.e.  $\pm 45^{\circ}$ ) were modelled using equivalent properties obtained from classical laminate theory, and are given in Table 1. In the case of the control joints, 69,650 bi-quadratic plane strain quadrilateral elements of type CPE8 were used. In the case of the vascularized joints, the mesh density was locally increased to account for the higher stress state at the periphery of the vasculature. There was a corresponding increase in the number of elements used to a maximum of 87,159 CPE8 elements. Convergence checks were performed to ensure sufficient mesh refinement was used. Failure was determined using the maximum transverse stress ( $\sigma_{tt}$ ) equation, as given in Eq.1. The maximum strength transverse to the fibers was assumed to be 92MPa [18].

$$\sigma_{tt_{90^{\circ}}} = \frac{\sigma_{22} + \sigma_{33}}{2} + \sqrt{\left(\frac{\sigma_{22} - \sigma_{33}}{2}\right)^2 + \tau_{23}^2} \quad (1)$$

The analysis was performed in two steps; first thermal loading was applied to the entire model before a combined mechanical and thermal loading was applied as described previously. Three different models were examined, an unvascularised control joint, a joint containing circular vasculature, and a joint containing TOPT vasculures.

### 2.2 Topology Optimisation

The topology of the optimised vasculature was determined using a series of manual iterative loops, each comprising of up to 12 individual analysis runs. The analysis was performed using the same two-step process as described in Section 2.1. For each analysis run, the location and magnitude of the peak stresses due to thermal loading only was recorded. This information was then collated and the geometry exhibiting the lowest thermal residual stresses was displayed using a simple ‘traffic light’ system (see Fig. 6). For the traffic-light system:

- Geometries exhibiting max transverse stresses in excess of 92MPa were deemed to have failed and are shown in red,
- Stresses from 70-92MPa are deemed to be at risk of failure and shown in orange,
- Stresses below 70MPa are arbitrarily deemed to be acceptable and shown in green.

The objective of the optimisation study was to maximise vascular cross sectional area whilst minimising peak stresses at the periphery of the vasculature. Starting with an arbitrary rectangular geometry with semi-elliptical ends (see Fig. 5), the width and elliptical aspect ratio were then varied. The purpose here was to determine an approximate maximum cross sectional area that could be achieved without exceeding the 70MPa “green” limit. The vasculature was positioned centrally at the bottom of the deltoid, nearest the substrate (see Fig. 1 for nomenclature). This location was selected as it was determined to be the most remote location within the deltoid from mechanically induced stresses. Once a first iteration of the design had been established, the topology was assessed under mechanical loading ( $U_2 = 2\text{mm}$ ). An acceptable geometry was one in which failure was expected to initiate remote from the vasculature during mechanical loading. Converging on such a geometry required a number of design loops, in which corners and stress concentrations around the vasculature periphery were smoothed and re-analysed.

After each design loop, a sensitivity analysis was performed to determine the maximum envelope for the effective placement of the vasculature. The sensitivity analysis involved moving the vasculature within the deltoid to determine the maximum X-Y translation and Z-rotation that could be accommodated for each geometry. A minimum manufacturing tolerance of 2mm X-translation, 0.375mm Y-translation (3 plies) and  $15^\circ$  Z-rotation. These limits were based on hand layout; further refinements may be achieved using automated manufacturing routes.

### 3 RESULTS & DISCUSSION

#### 3.1 Control & Circular Analysis

In order to determine the stress state within the deltoid and surrounding regions, a control analysis was performed. It can be seen from Fig. 3 that the stress state within the deltoid varies from a maximum of 49.2MPa at the deltoid tips, to a transverse stress-free state at the centroid. From this analysis it can be concluded that the most logical location in which to locate a vascular feature, such that it experiences minimal thermal stress concentrations, would be at this centroid location.

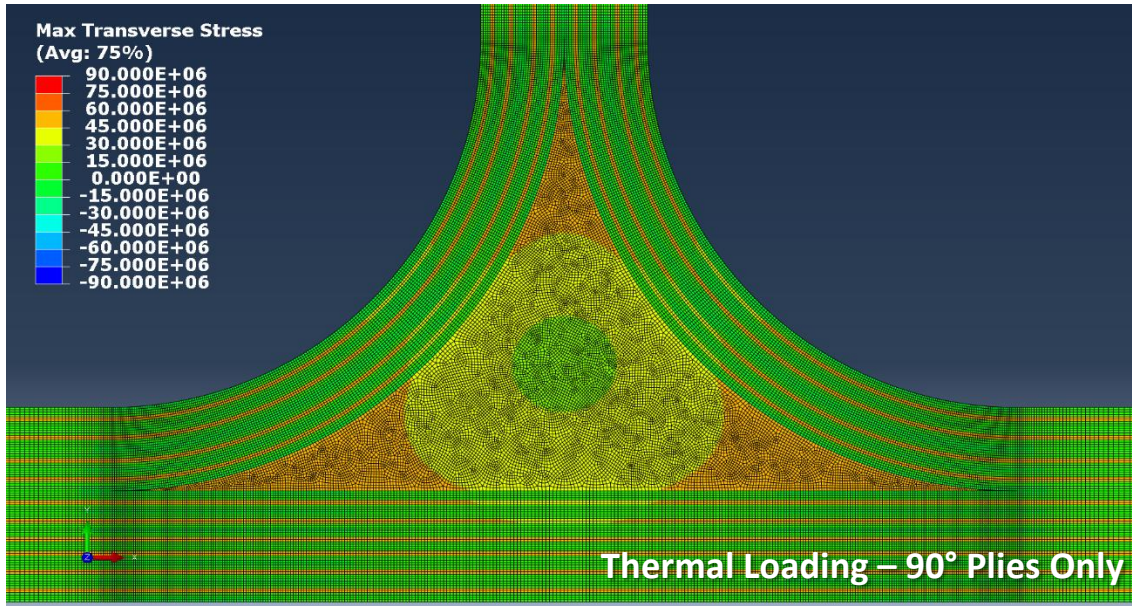


Figure 3: Thermal residual stress state within deltoid region due to thermal loading.

Next, the influence of combined thermal and mechanical loading on the stress state within the deltoid was assessed and presented in Fig. 4. Firstly it can be noted that as the vertical displacement increases, the regions of the deltoid at the root of the curved overlaminated section become most highly stressed. It can also be seen that the centre of the deltoid experiences high maximum transverse stresses, increasing with vertical displacement. Comparing Figures 3 and 4 it can be concluded that the optimal location for vasculature deployment is non-obvious, requiring trade-off between locations and topology optimisation.



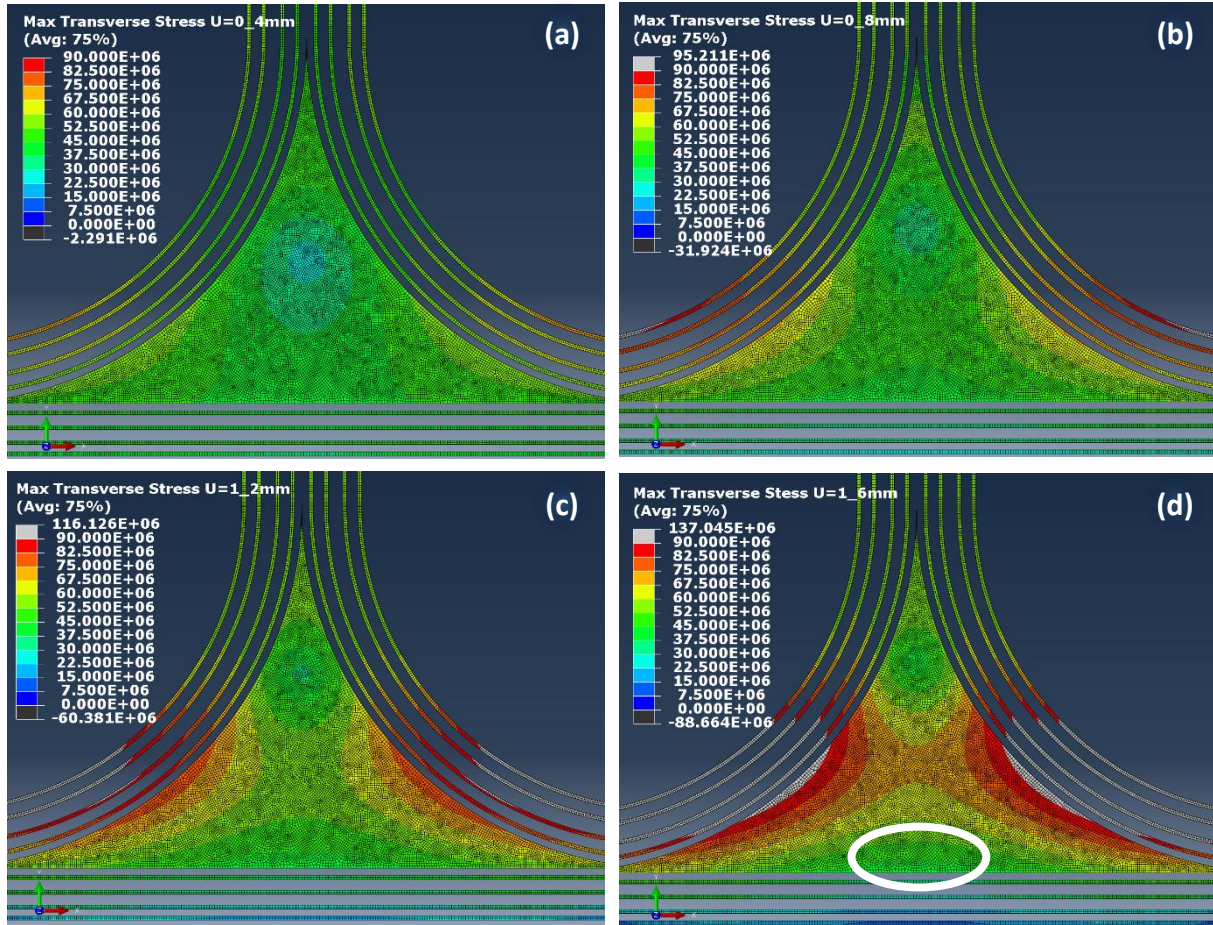


Figure 4: Stress evolution during combined thermal /mechanical loading ( $U_2$ ), 90° plies  
(a)  $U_2 = 0.4\text{mm}$  (b)  $U_2 = 0.8\text{mm}$  (c)  $U_2 = 1.2\text{mm}$  (d)  $U_2 = 1.6\text{mm}$ , potential vasculature deployment region

One potential location that would satisfy both thermal and mechanical loading, would be to deploy vasculature centrally at the base of the deltoid, adjacent to the deltoid/substrate interface as shown in Fig. 4(d). This region experiences thermal stresses of the order of 30-40MPa, and combined stresses of the order of 40-50MPa (at  $U_2 = 2\text{mm}$ ). Another advantage of this region is ease of manufacturing. As the deltoid regions are manufactured using hand layup, accurate placement of vasculature can be challenging. Placement on or near the deltoid/substrate interface, however, is significantly less problematic than placement at an arbitrary location within the deltoid.

A preliminary analysis of circular vasculature was performed to assess the suitability of the aforementioned location for vasculature deployment. A 1mm diameter vasculature was located 0.250mm (2 x plies) from the bottom of the deltoid. Under thermal loading a  $\sigma_{tt}$  of 106.3MPa was observed at the periphery of the vasculature, increasing to 137.5MPa at 1.6mm displacement. At these stress levels, the structure would not be expected to survive autoclave processing, and if it did, would be likely to fail prematurely under mechanical loading. It is clear that this location has potential, however circular vasculature is not suitable for such high temperature manufacturing.

### 3.2 Topology Optimisation (TOPT) Analyses

As mentioned previously, the objective of the optimisation study was to maximise vascular cross sectional area whilst minimising peak stresses at the periphery of the vasculatures. To achieve this, an initial width of 2mm and parabolic aspect ratio ( $B/h$ ) of 1.11 were selected (see Figs. 6 & 7). From here the topology was subject to three design loop iterations. The model was subject to thermal and combined thermal/mechanical loads as described previously. Topology iteration was ceased when improvements per cycle fell below 1MPa. For the purposes of this parametric study this was deemed to be sufficient.

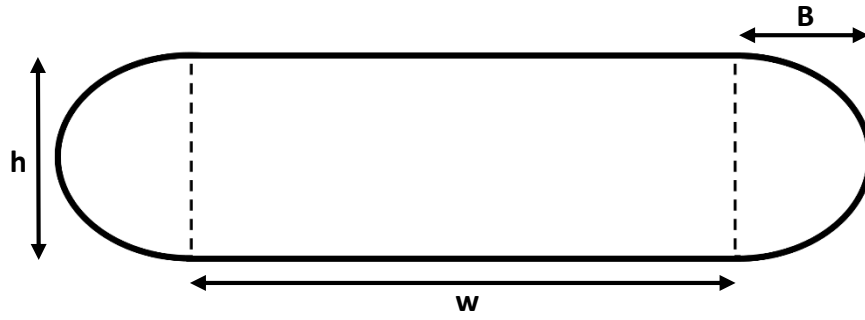


Figure 5: Initial profile for topology optimisation (TOPT)

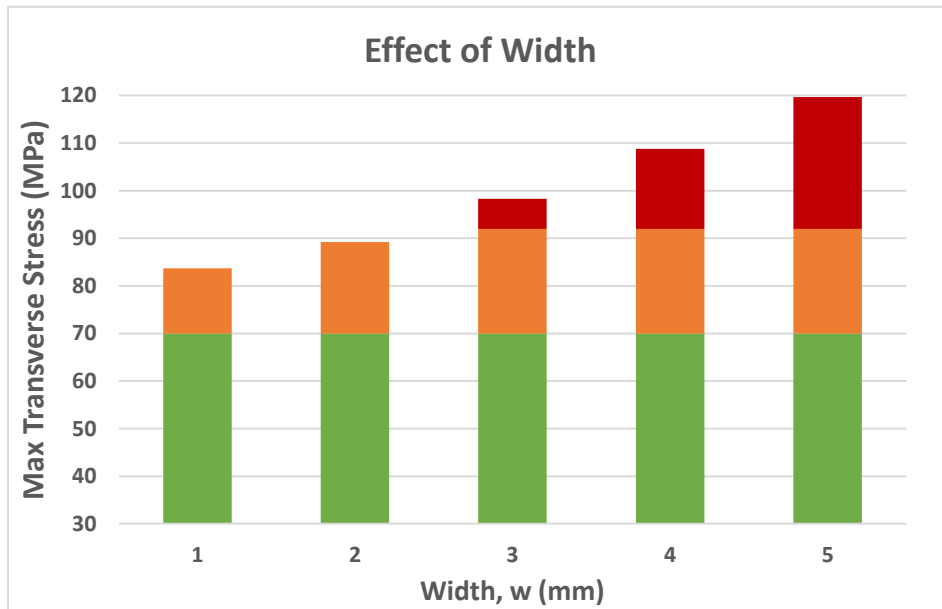


Figure 6: Effect of width on thermal residual stresses ( $\sigma_{tt}$ ) at vasculature periphery,  $h = 0.5\text{mm}$ ,  $B/h = 2$

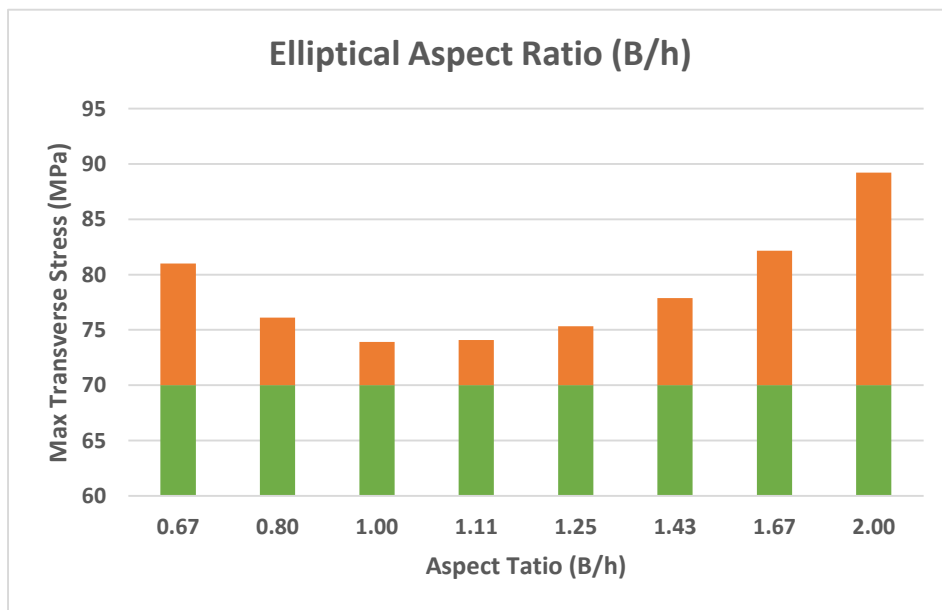


Figure 7: Effect of elliptical aspect ratio on thermal residual stresses ( $\sigma_{tt}$ ) at vasculature periphery,  $h = 0.5$ ,  $w = 2\text{mm}$

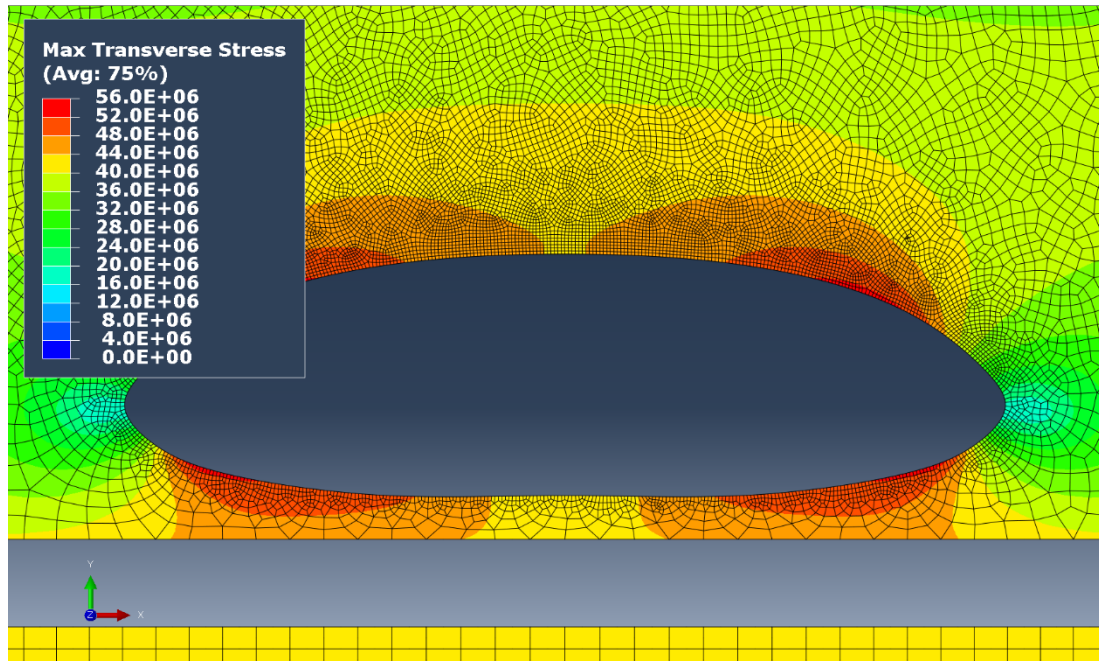


Figure 8: Thermal residual stress state within deltoid region due to thermal loading.

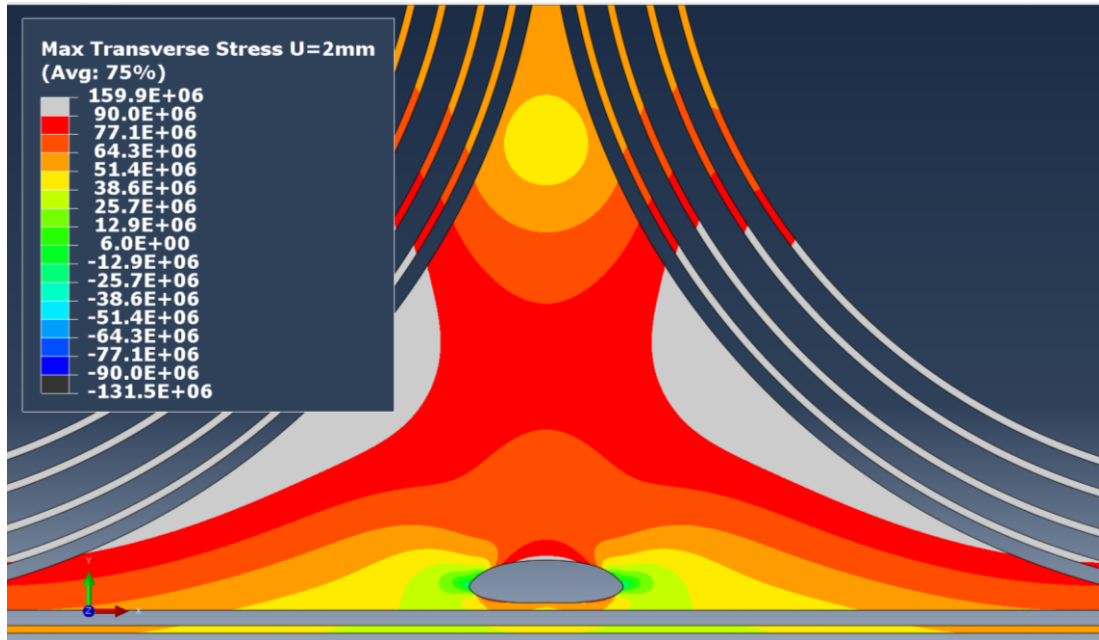


Figure 9: Failure in TOPT specimen anticipated to occur remote from vasculature location, thermal & mechanical loading,  $U_2=2\text{mm}$ , (mesh removed from image for visualisation purposes).

After a series of design loop iterations and sensitivity studies, a final topology was established that met the design criterion for the geometry/load cases presented. Under thermal loading, a maximum thermal  $\sigma_{tt}$  of 54.1MPa was achieved. Examining Fig. 9, it can be seen that under combined loading it is anticipated that failure would be expected to occur at the root of the overlaminates, as per the control analysis (Fig. 4), prior to initiating at the vasculature. The proposed topology achieves a 49% reduction in thermal residual stresses at the vasculature periphery. In addition, a 3.5x increase in cross sectional area and 7.16x increase in vasculature surface area is achieved compared to the largest channels successfully implemented in self-healing found in the literature [12–14,16,22,23].



## 4 CONCLUSIONS

A simple but robust method for the optimisation of vasculature (embedded hollow channels) for deployment in self-healing fibre reinforced polymer structures has been presented. The T-joint geometry was selected for this study as it is a widely used industrial configuration and is a design feature which lends itself well to the introduction of a vasculature network. 2D thermoelastic finite element analysis revealed that conventional circular vasculature are ill-suited to deployment in complex structures due to stress concentrations around the periphery. Instead, an optimised topology was determined which significantly decreased stress concentrations to acceptable levels, whilst simultaneously allowing for greatly increased vasculature dimensions. The ability to introduce large vasculature infrastructure into a component may also be desirable for other smart applications such as structural health monitoring and thermal management.

The overall objective of implementing self-healing / in-situ repair technology into composite structural features is to expand the allowable damage envelope for engineers. It is hoped that this technology will ultimately improve the safety of primary structures, whilst mitigating the need for costly repairs.

## ACKNOWLEDGEMENTS

The authors would like to acknowledge the support of our European partners within SHeMat for their time and contributions. This research was sponsored by the People Program (Marie Curie ITN) of the European Union's seventh framework program, FP7, grant number 290308 (SHeMat).

## REFERENCES

- [1] Katnam KB, Da Silva LFM, Young TM. Bonded repair of composite aircraft structures: A review of scientific challenges and opportunities. *Prog Aerosp Sci* 2013;61:26–42. doi:10.1016/j.paerosci.2013.03.003.
- [2] Park H, Kong C. Experimental study on barely visible impact damage and visible impact damage for repair of small aircraft composite structure. *Aerosp Sci Technol* 2013;29:363–72. doi:10.1016/j.ast.2013.04.007.
- [3] White SR, Sottos NR, Geubelle PH, Moore JS, Kessler MR, Sriram SR, et al. Autonomic healing of polymer composites. *Nature* 2001;409:794–7. doi:10.1038/35057232.
- [4] Kessler M, White S. Self-activated healing of delamination damage in woven composites. *Compos Part A Appl Sci Manuf* 2001;32:683–99. doi:10.1016/S1359-835X(00)00149-4.
- [5] Kessler M., Sottos N., White S. Self-healing structural composite materials. *Compos Part A Appl Sci Manuf* 2003;34:743–53. doi:10.1016/S1359-835X(03)00138-6.
- [6] O'Brien T. Assessment of Composite Delamination Self-Healing Under Cyclic Loading. ICCM-17 17th Int Conf Compos Mater 2009.
- [7] Bleay S., Loader C., Hawyes V., Humberstone L, Curtis P. A smart repair system for polymer matrix composites. *Compos Part A Appl Sci Manuf* 2001;32:1767–76. doi:10.1016/S1359-835X(01)00020-3.
- [8] Trask RS, Bond IP. Biomimetic self-healing of advanced composite structures using hollow glass fibres. *Smart Mater Struct* 2006;15:704–10. doi:10.1088/0964-1726/15/3/005.
- [9] Huang C-Y, Trask RS, Bond IP. Characterization and analysis of carbon fibre-reinforced polymer composite laminates with embedded circular vasculature. *J R Soc Interface* 2010;7:1229–41. doi:10.1098/rsif.2009.0534.
- [10] Zako M, Takano N. Intelligent Material Systems Using Epoxy Particles to Repair Microcracks and Delamination Damage in GFRP. *J Intell Mater Syst Struct* 1999;10:836–41. doi:10.1106/YEIH-QUDH-FC7W-4QFM.
- [11] Meure S, Wu DY, Furman S. Polyethylene-co-methacrylic acid healing agents for mendable epoxy resins. *Acta Mater* 2009;57:4312–20. doi:10.1016/j.actamat.2009.05.032.

- [12] Norris CJ, Bond IP, Trask RS. The role of embedded bioinspired vasculature on damage formation in self-healing carbon fibre reinforced composites. *Compos Part A Appl Sci Manuf* 2011;42:639–48. doi:10.1016/j.compositesa.2011.02.003.
- [13] Norris CJ, Meadway GJ, O’Sullivan MJ, Bond IP, Trask RS. Self-Healing Fibre Reinforced Composites via a Bioinspired Vasculature. *Adv Funct Mater* 2011;21:3624–33. doi:10.1002/adfm.201101100.
- [14] Norris CJ, Bond IP, Trask RS. Interactions between propagating cracks and bioinspired self-healing vasculature embedded in glass fibre reinforced composites. *Compos Sci Technol* 2011;71:847–53. doi:10.1016/j.compscitech.2011.01.027.
- [15] Norris CJ, Bond IP, Trask RS. Healing of low-velocity impact damage in vascularised composites. *Compos Part A Appl Sci Manuf* 2013;44:78–85. doi:10.1016/j.compositesa.2012.08.022.
- [16] Norris CJ, White JAP, McCombe G, Chatterjee P, Bond IP, Trask RS. Autonomous stimulus triggered self-healing in smart structural composites. *Smart Mater Struct* 2012;21:094027. doi:10.1088/0964-1726/21/9/094027.
- [17] Trask RS, Hallett SR, Helenon FMM, Wisnom MR. Influence of process induced defects on the failure of composite T-joint specimens. *Compos Part A Appl Sci Manuf* 2012;43:748–57. doi:10.1016/j.compositesa.2011.12.021.
- [18] Hélénon F, Wisnom MR, Hallett SR, Trask RS. Numerical investigation into failure of laminated composite T-piece specimens under tensile loading. *Compos Part A Appl Sci Manuf* 2012;43:1017–27. doi:10.1016/j.compositesa.2012.02.010.
- [19] Hélénon F, Wisnom MR, Hallett SR, Trask RS. Investigation into failure of laminated composite T-piece specimens under bending loading. *Compos Part A Appl Sci Manuf* 2013;54:182–9. doi:10.1016/j.compositesa.2013.07.015.
- [20] Cullinan JF, Wisnom M, Bond I. A Novel Method for the Manipulation of Damage and In-Situ Repair of Composite T-Joints. 56th AIAA/ASCE/AHS/ASC Struct. Struct. Dyn. Mater. Conf., Reston, Virginia: American Institute of Aeronautics and Astronautics; 2015, p. 1–10. doi:10.2514/6.2015-1577.
- [21] Jiang W-G, Hallett SR, Green BG, Wisnom MR. A concise interface constitutive law for analysis of delamination and splitting in composite materials and its application to scaled notched tensile specimens. *Int J Numer Methods Eng* 2007;69:1982–95. doi:10.1002/nme.1842.
- [22] Hamilton AR, Sottos NR, White SR. Self-healing of internal damage in synthetic vascular materials. *Adv Mater* 2010;22:5159–63. doi:10.1002/adma.201002561.
- [23] Hamilton AR, Sottos NR, White SR. Mitigation of fatigue damage in self-healing vascular materials. *Polymer (Guildf)* 2012;53:5575–81. doi:10.1016/j.polymer.2012.09.050.